BIODIVERSITAS
Volume 26, Number 3, March 2025
Pages: 1180-1188

ISSN: 1412-033X
E-ISSN: 2085-4722
DOI: 10.13057/biodiv/d260317

Mapping coral reefs growth using drone imagery in Gili Labak Island, Sumenep District, East Java, Indonesia

FIRMAN FARID MUHSONI[1,♥], ADNIN TAMHIDA SHOBRINA SALSABIL[1], SAFA[1], MUHAMMAD ZAINURI[1], ABU BAKAR SAMBA[2], ELYS FAUZYAH[3], DEDI IRAWAN[1]

[1]Program of Water Resource Management, Faculty of Agriculture, Universitas Trunojoyo Madura. Jl. Raya Telang, PO. Box. 2 Kamal, Bangkalan 69162, East Java, Indonesia. Tel./fax.: +62-31-3011146, ♥email: firmanfaridmuhsoni@trunojoyo.ac.id
[2]Faculty of Fisheries and Marine Science, Universitas Brawijaya. Jl. Veteran, Ketawanggede, Lowokwaru, Malang 65145, East Java, Indonesia
[3]Program of Agribusiness, Faculty of Agriculture, Universitas Trunojoyo Madura. Jl. Raya Telang, PO. Box. 2 Kamal, Bangkalan 69162, East Java, Indonesia

Manuscript received: 9 September 2024. Revision accepted: 7 March 2025.

Abstract. *Muhsoni FF, Salsabil ATS, Safa, Zainuri M, Samba AB, Fauzyah E, Irawan D. 2025. Mapping coral reefs growth using drone imagery in Gili Labak Island, Sumenep District, East Java, Indonesia. Biodiversitas 26: 1180-1188.* The benthic habitat serves as the dwelling place for diverse aquatic organisms, primarily characterized by coral reefs. Meanwhile, Gili Labak Island, Sumenep District, East Java, Indonesia has a well-preserved marine ecosystem, including coral reefs, seagrass beds, and other marine organisms. A drone is one of the platforms that can be used to map benthic habitats, which has the advantages of relatively low cost, the ability to monitor temporal changes over a short period, and the capacity to use multispectral sensors. In this research, drone imagery or Unmanned Aerial vehicles from 2021 and 2022 were used. The classification method used was the supervised maximum likelihood, and accuracy testing was conducted using a confusion matrix. In addition, coral reef cover data was directly collected using the Underwater Photo Transect (UPT) method in September 2023. The classification results using the supervised maximum likelihood method with drone imagery were able to identify changes in coral reefs from 2021 to 2022. The accuracy test results showed an overall accuracy ranging from 74.20% to 86.47% (2021 data) and 79.94% to 90.87% (2022 data). The kappa coefficient values obtained were 71.80% to 82.72% (2021 data) and 70.33% to 89.25% for 2022 data. Drone imagery has proven to be useful in observing coral growth through changes in coverage. In this study, changes in live coral coverage (Acropora, Goniastrea, Mycedium, Pocillopora, Porites, and Stylophora) between 2021 and 2022 were observed. At Station 1, the coral coverage increased from 176.77 m² (30.95%) to 323.18 m² (57.43%). At Station 2, it decreased from 740.25 m² (75.21%) to 462.61 m² (47.68%). At Station 3, it decreased from 422.11 m² (94.91%) to 377.44 m² (86.26%). The percentage of coral reef cover using the average Underwater Photo Transect (UPT) method was 61.66%. This study demonstrates that the application of high-resolution drone imagery, along with mapping and monitoring methods, can be used to detect changes in coral reef conditions, providing valuable information for management and conservation strategies.

Keywords: Coral growth, drone, Gili Labak, supervised maximum likelihood, underwater photo transect

INTRODUCTION

The global benthic ecosystem has been affected by human activities, such as land-based pollution, over-exploitation, coastal modifications, ocean acidification, and climate change (Storlazzi et al. 2017; Oberle et al. 2019; Takesue and Storlazzi 2019). It is important to establish a precise geospatial inventory for the benthic system, tracking the structural and compositional evolution over time. Key components of this monitoring include creating accurate maps of species distribution, health conditions, and species diversity, closely related to fundamental marine features such as reefs, rocks, debris, and sand (Roelfsema et al. 2018; Magel et al. 2019). Data and information on the condition of coral reefs over time are crucial for determining the appropriate conservation strategies.

Coral reef monitoring methods include in situ surveys and the analysis of remote sensing data from satellites. In situ methods are often costly and inconsistent in terms of time and space (Hedley et al. 2016; Bennett et al. 2020; Vitousek et al. 2023). Various methods are used to monitor benthic habitat and substrate features, specifically in coral reefs. These methods include field observations Reverter et al. (2022) LiDAR mapping three-dimensional structures of coral reefs community (Wedding et al. 2019), multispectral satellite image analysis (Li et al. 2020; Wei et al. 2020; Sativa et al. 2021), 3D photo methods (Burns et al. 2019; Fukunaga et al. 2019; Irawan et al. 2023), use of Autonomous Underwater Vehicles (Yu et al. 2021), and the latest development including drone.

According to Kabiri et al. (2020) field observation is the most accurate but costly and only feasible for small areas. Meanwhile, the use of satellite remote sensing images can cover large areas but with lower accuracy. The use of remote sensing with drones has emerged as an effective alternative solution. Drone-based imagery can be used to classify bleached and non-bleached corals (Giles et al. 2023). Drone imagery facilities can be used to monitor temporal changes in coral reefs complexity, providing multispectral data and bathymetry in shallow water coral reefs, with an accuracy of -0.016±0.45 m. In contrast to field observations, drone imagery can distinguish coral types including bleached coral and other substrate characteristics over a relatively large area in a short period.

This method requires lower costs than field observations and provides more accurate results compared to satellite imagery (Kabiri et al. 2020).

Indonesia has numerous islands with vast coral reef potential, one of which is Gili Labak Island, Sumenep District, East Java. In situ monitoring surveys would require significant financial resources. The use of drones can offer an effective and economical solution to address this issue. The aim of this research is to map coral reef changes over different years using a commercial drone and to determine the coral reef cover. The study location is Gili Labak Island, Sumenep District, East Java Province, Indonesia. This study utilized drone imagery to map coral reef conditions by comparing images captured in 2021 and 2022. The drone data were processed using a supervised classification method to determine coral cover for each year. The results were then compared with and validated against field data collected using the Underwater Photo Transect (UPT) method. The objectives of this study were (i) to measure coral growth from 2021 to 2022 using drone imagery; (ii) to evaluate the accuracy of drone-based coral reef mapping through supervised maximum likelihood classification; (iii) to determine the in situ percentage of coral reef cover using the UPT method as a comparison. This study develops a coral reef mapping method to address the limitations of satellite imagery, which has so far been less effective. The advantage of using drones is that data can be collected at any time as needed, and drone images offer very high spatial resolution. This makes it easier to monitor coral reef conditions within a limited area.

MATERIALS AND METHODS

Study area

This research was conducted on Gili Labak Island, Sumenep District, East Java, Indonesia geographically located at coordinates 7°11'59"S-7°12'34"S and 114°2'34"E-114°3'7"E. Data collection was carried out in September 2021 and October 2022 (Figure 1). Coral reef area on Gili Labak Island 0.5 km^2. Subsequently, coral on Gili Labak was previously surveyed using various methods, including field observations (Insafitri et al. 2021), and 3D photo methods (Irawan et al. 2023). This study utilized a DJI Phantom 4 drone, Underwater Photo Transect (UPT) data collection with an Olympus TG-6 camera, and drone analysis using Agisoft Metashape, ENVI, and ArcGIS software.

Procedures

In the initial stages of flight path planning, key steps include determining the planned flight area, establishing sidelap and overlap, calculating the number of photos, planning take-off and landing locations, and setting drone's flying altitude (Sanfourche et al. 2015). Aerial photo capture is strategically scheduled for the late afternoon to avoid sunlight that may degrade image quality and take advantage of low tide conditions in seawater. The drone imagery was captured in the western region of Gili Labak Island, as this location is where snorkeling activities are frequently conducted.

In addition to drone data, this study also collected field data using the underwater photo transect (UPT) method. Schaduw et al. (2020) and Jericho et al. (2023) explained that the UPT method involves photographing underwater substrates using an underwater camera positioned perpendicular to the substrate. Each photo uses a frame measuring 58×44 cm as a quadrant. Photos are taken along a 50-meter transect, with one photo captured every meter, resulting in a total of 50 frames (photos) (Figure 2). These photos are then analyzed using the Coral Point Count with Excel (CPCe) software.

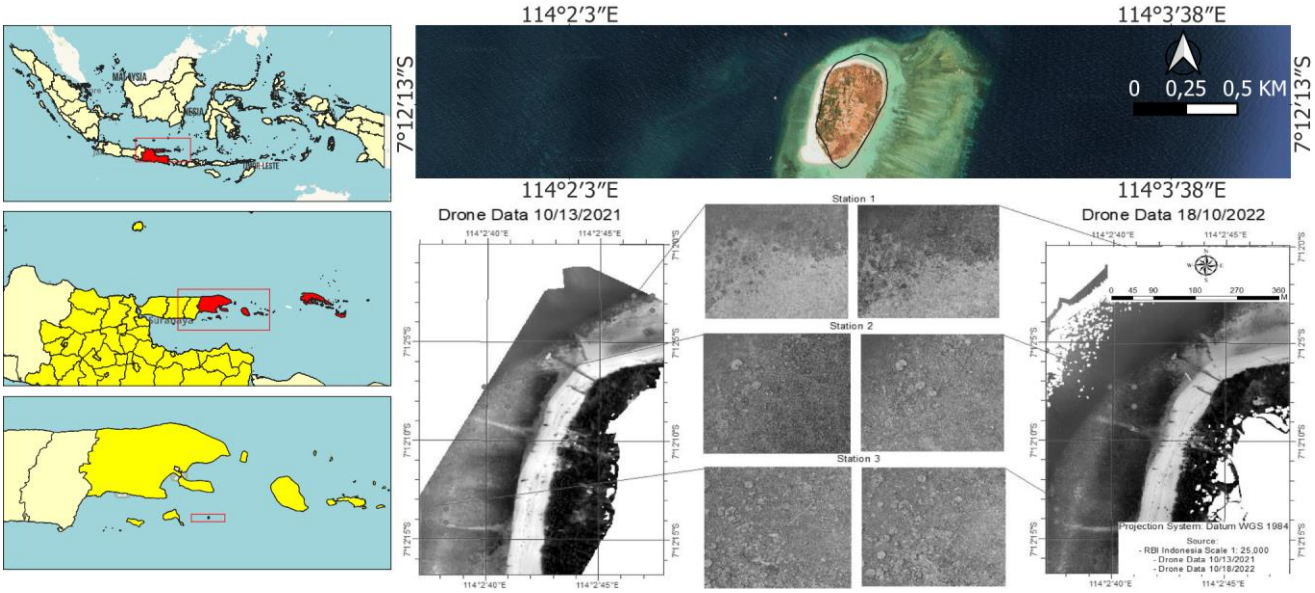

Figure 1. Research location in Gili Labak Island, Sumenep District, East Java, Indonesia

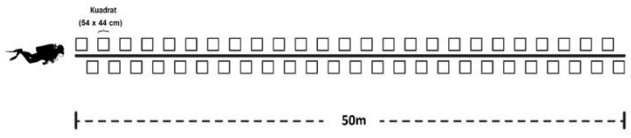

Figure 2. Illustration of coral reef observation using the Underwater Photo Transect (UPT) method (Hidayat et al. 2023)

Data analysis

de Oliveira et al. (2021), Fukunaga et al. (2019), and Urbina-Barreto et al. (2021) describe the analysis of drone photos with the following steps: (i) Estimating the quality of underwater images based on sharpness, exposure, focus, resolution, and depth of field; (ii) calibrating the camera and building a dense cloud using software; (iii) scaling using a scale factor; (iv) constructing a dense point cloud with depth information for each camera and densification algorithm; (v) building a 3D network Build Texture (optional).

Following image acquisition, drone results were classified using the supervised classification with the maximum likelihood algorithm. In Machine Learning (ML), the distribution for each class in each band is assumed to be normal, and the probability of a given pixel belonging to a specific class is calculated. Each pixel is then assigned to the class with the highest probability. Classification is performed by calculating the discriminant function for each pixel in the image (Ahmad et al. 2018; Peng et al. 2018). The classification process begins with creating training samples or Region of Interest (ROI) used to define classes of coral reefs cover. The accuracy of the classification results was assessed using a confusion matrix (Ventura et al. 2016; Ruwaimana et al. 2018).

The collected photos are then analyzed using a computer program (application) called Coral Point Count Excel (CPCe) (Schaduw et al. 2020; Jericho et al. 2023). This method is also referred to as the underwater digital photogrammetry protocol (UWP) (Barrera-Falcon et al. 2021) or the Photo Line Intercept Transect (PLIT) (Nakajima et al. 2010).

RESULTS AND DISCUSSION

Coral reef mapping using drones

The resulting orthophoto showed a comprehensive overview of the compilation of aerial photos obtained. The merged aerial photos have a resolution of 5472x3648, a pixel size of 2.41x2.41 µm, and a ground resolution of 2.08 cm/pixel (18/10/2022) and 2.29 cm/pixel (13/10/2021). The flying altitude was 85.2 m (18/10/2022) and 92.3 m (13/10/2021). The pixel value from drone image shows the area captured within one pixel, with each pixel representing an area of 2.08 cm^2 or 2.29 cm^2. The drone imagery processed using Agisoft Metashape produced Root Mean Square Error (RMSE) values, a parameter used to evaluate the spatial accuracy of drone data processing (lkhrachy 2021; Žabota and Kobal 2021). In Table 1, RMSE is calculated for the X, Y, and Z directions, as well as for the total error. For the data collected on October 18, 2022, the X error was 2.75 m, Y error was 0.79 m, Z error was 1.36 m, XY error was 2.86 m, and the total error was 3.16 m. The largest error occurred in the X direction. For the data collected on October 13, 2021, the X error was 2.50 m, Y error was 2.92 m, Z error was 1.14 m, XY error was 3.84 m, and the total error was 4.01 m. The largest error occurred in the Y direction. The drone imagery mapping on October 18, 2022, was more accurate due to improved processing techniques, an adequate number of GCPs, and stable flight conditions. Martínez-Carricondo et al. (2018) found that stratified GCP distribution within the study area, with a density of approximately 0.5-1 GCP×ha^{-1}, minimizes altimetric errors. Zhong et al. (2025) explained that a high GCP density exceeding 10 GCP/km^2 results in RMSE values as low as 0.1 m.

The image cropping process is directed at concentrating on the specific area for classification. The designated cropping locations include Station 1, situated close to the pier and other structures. Station 2 is located beside the pier and is used for tourist activities such as diving and snorkeling. Station 3 is positioned farther away from tourist activities (Figure 1). The under classification of drone images shows distinct extents and distributions of coral reefs each year at Station 1. The classification results include 8 classes, namely Acropora, algae, Goniastrea, Micedium, Porites, rubble, sand, and Stylopora (Figure 3). The classification results at Station 1 show the highest percentage of rubble. In 2021, the rubble area measured 204.60 m^2 or approximately 35.82%, while in 2022, it decreased to 140.17 m^2, constituting around 24.91% (Table 2). The most commonly found coral species at Station 1 is Acropora. The classifications categorized as live corals at Station 1 include Acropora, Goniastrea, Mycedium, Porites, and Stylophora. In 2021, live coral coverage reached 176.77 m^2 (30.95%), while in 2022, it increased to 323.18 m^2 (57.43%). This indicates an expansion of live coral coverage at Station 1 by 146.41 m^2 or 26.48%. The most significant increase was observed in Porites coral, which grew from 5.38-14.55%. The rapid growth of Porites is attributed to its ability to survive under various unfavorable environmental conditions, such as high sedimentation and salinity fluctuations.

The classification results at Station 2 include 9 classes, namely Acropora, algae, Goniastrea, Mycedium, Pocillopora, Porites, rubble, sand, and Stylopora (Figure 4). The classifications categorized as live corals at Station 2 include Acropora, Goniastrea, Mycedium, Pocillopora, Porites, and Stylophora. In 2021, live coral coverage reached 740.25 m^2 (75.21%), while in 2022, it decreased to 462.61 m^2 (47.68%). This indicates a decline in live coral coverage at Station 2 by 277.64 m^2 or 27.53%. The most significant reduction was observed in Acropora, which decreased by 172.63 m^2 (17.39%). The Goniastrea coral decreased by 3.13 m^2 (0.21%), Mycedium by 64.38 m^2 (6.50%), Pocillopora by 5.44 m^2 (0.55%), Porites by 22.78 m^2 (1.97%), and Stylophora by 9.28 m^2 (0.91%). Meanwhile, rubble at Station 2 increased by 289.05 m^2 (30.07%), indicating significant coral damage. The increase in the rubble area at Station 2 is due to its proximity to the

pier, where coral reefs often suffer damage due to anchor use. Porites coral is a prevalent type, along with Acropora coral. In 2021, the area of Porites coral was 251.28 m^2 or approximately 25.53%, and in 2022, it was 228.50 m^2 or approximately 23.55%. Meanwhile, Acropora coral in 2021 covered an area of 273.61 m^2 or about 27.80%, and in 2022, it covered an area of 100.98 m^2 or about 10.41% (see Table 2). The decline in both Porites and Acropora corals suggests coral reefs mortality, possibly influenced by factors such as water quality and human activities. Station 2 is a popular spot for tourists to snorkel, contributing to the increasing damage to coral reefs.

At Station 3, the classification consisted of 8, including Acropora, algae, Goniastrea, Mycedium, Porites, rubble, sand, and Stylopora (Figure 5). The classifications categorized as live corals at Station 3 include Acropora, Goniastrea, Mycedium, Porites, and Stylophora. In 2021, live coral coverage reached 422.11 m^2 (94.92%), while in 2022, it decreased to 377.44 m^2 (86.26%). Although live coral coverage at Station 3 remained high, it showed a reduction of 44.67 m^2 or 8.66%. The most significant decline was observed in Acropora, which decreased by 93.10 m^2 (20.71%). On the other hand, Goniastrea increased by 18.11 m^2 (4.39%), Mycedium increased by 21.53 m^2 (5.09%), and Porites increased by 52.69 m^2 (12.28%). However, Stylophora experienced a decline of 43.90 m^2 (9.70%). Meanwhile, rubble at Station 3 increased by 37.32 m^2 (8.57%), indicating some coral damage, although the extent was less severe than at Station 2. The results show Porites coral as the most prevalent type, experiencing an increase in 2022. In 2021, the area of porites coral was 63.57 m^2 or approximately 14.30%, and in 2022, it was 116.26 m^2 or about 26.57%. On the other hand, Acropora coral decreased, with an area of 154.11 m^2 or approximately 34.66% in 2021 and 61.01 m^2 or 13.94% in 2022 (Table 2). The decline in Acropora may be attributed to growth of other coral types. The classification results for Station 3 show that there are still large areas of coral reefs such as Goniastrea, Micedium, and Stylophora, each covering more than 10%. Limited tourist activities at Station 3 also contribute to the high percentage of coral reefs in this area. The smallest class area is sand, measuring 5.12 m^2 or about 1.15% in 2021 and 0.78 m^2 or approximately 0.18% in 2022.

The accuracy test using a confusion matrix, at Station 1 resulted in an overall accuracy of 80.49% and 90.87% for the classifications in 2021 and 2022, respectively. The kappa coefficient values obtained at Station 1 were 76.44% and 89.25% for the classifications in 2021 and 2022, respectively. Station 2 produced overall accuracy values of 86.47% and 79.94% for the classifications in 2021 and 2022. The kappa coefficient values at Station 2 were 82.72% and 70.33% for the classifications in 2021 and 2022, respectively. For Station 3, the overall accuracy values were 74.20% and 86.55% for the classifications in 2021 and 2022. The kappa coefficient values at Station 3 were 71.80% and 82.64% for the classifications in 2021 and 2022, respectively.

Percentage of coral cover using the underwater photo transect method

The coral reef cover results from field surveys using the Underwater Photo Transect (UPT) method showed that at Station 1 (Figure 6), Hard Coral Life was 54.94%, Soft Coral 0.07%, Others 0.47%, Mobile Substrate 16.44%, and Available Substrate 28.8% (Table 3). The hard coral details comprised 9 types: Acrpora Branching (ACB) 30.61%, Acropora Digitate (ACD) 0.94%, Acropora Submassive (ACS) 5.61%, Coral Branching (CB) 4.88%, Coral Encrusting (CE) 0.13%, Coral Foliose (CF) 3.14%, Coral Massive (CM) 7.09%, Coral Mushroom (CMR) 2.01%, and Coral Submassive (CS) 0.53%. At Station 2, Hard Coral Life was 81.76%, Soft Coral 2.75%, Others 2.75%, Mobile Substrate 7.13%, and Available Substrate 6.86% (Table 2).

Table 1. RMSE of Agisoft Metashape

	X error (m)	Y error (m)	Z error (m)	XY error (m)	Total error
18/10/2022	2.75	0.79	1.36	2.86	3.16
13/10/2021	2.50	2.92	1.14	3.84	4.01

Table 2. Coral reefs classification for 2021 and 2022

Class	Wide (m^2)		Percentage (%)	
	Year 2021	Year 2022	Year 2021	Year 2022
Station 1				
Acropora	68.72	97.42	12.03	17.31
Algae	40.63	50.65	7.11	9.00
Goniastrea	37.24	39.98	6.52	7.10
Mycedium	17.13	23.69	3.00	4.21
Sand	149.16	48.78	26.12	8.67
Porites	30.72	112.14	5.38	19.93
Rabble	204.60	140.17	35.82	24.91
Stylophora	22.96	49.95	4.02	8.88
Station 2				
Acropora	273.61	100.98	27.80	10.41
Algae	34.19	28.39	3.47	2.93
Goniastrea	76.94	73.81	7.82	7.61
Mycedium	93.89	29.51	9.54	3.04
Sand	24.96	5.15	2.54	0.53
Pocillopora	9.99	4.55	1.01	0.47
Porites	251.28	228.50	25.53	23.55
Rabble	184.88	473.93	18.78	48.85
Stylophora	34.54	25.26	3.51	2.60
Station 3				
Acropora	154.11	61.01	34.66	13.94
Algae	5.63	10.18	1.27	2.33
Goniastrea	67.08	85.19	15.09	19.47
Mycedium	46.93	68.46	10.55	15.65
Sand	5.12	0.78	1.15	0.18
Porites	63.57	116.26	14.30	26.57
Rabble	11.82	49.14	2.66	11.23
Stylophora	90.42	46.52	20.33	10.63

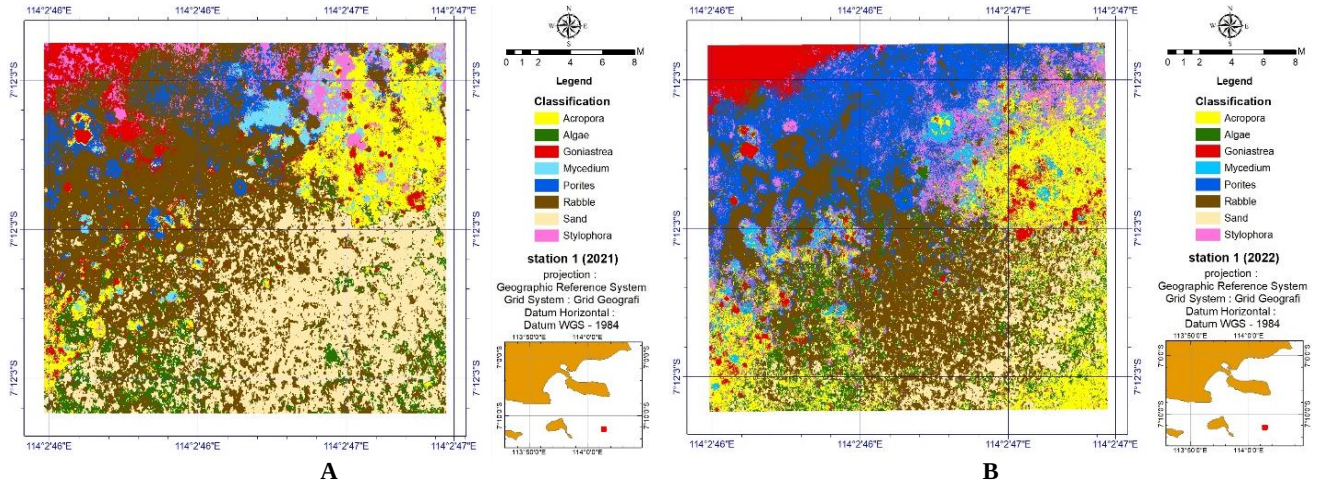

Figure 3. A. Station classification results 1 in 2021; B. Station classification results 1 in 2022

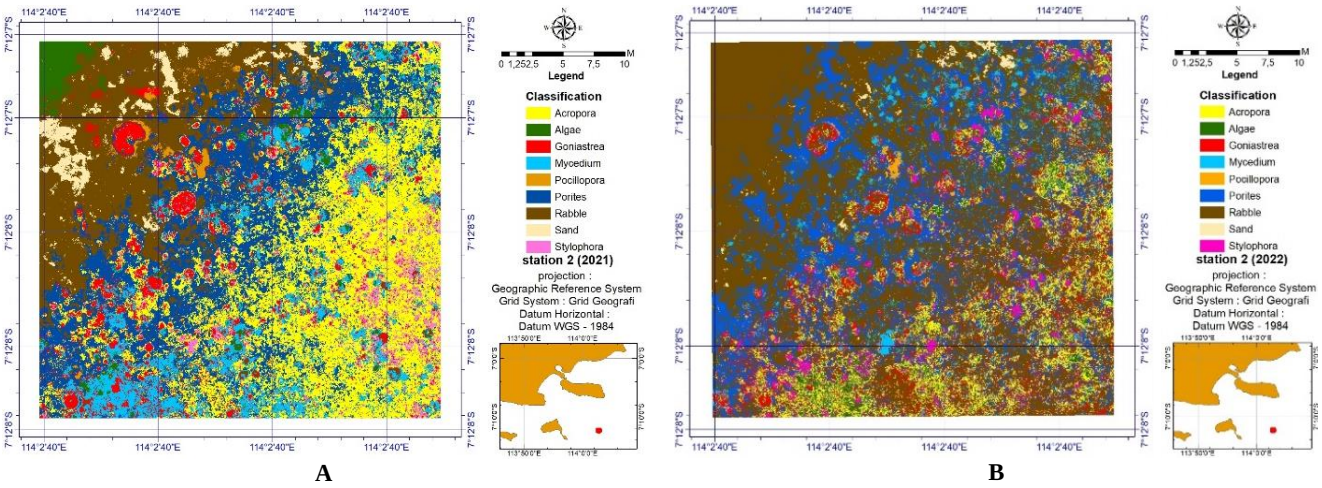

Figure 4. A. Station classification results 2 in 2021; B. Station classification results 2 in 2022

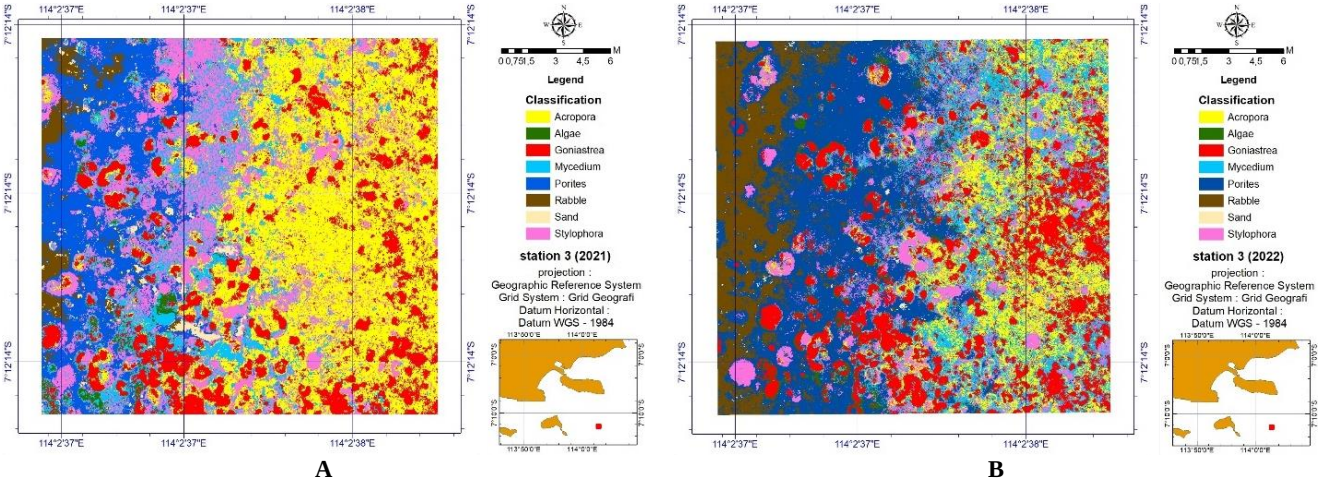

Figure 5. A. Station classification results 3 in 2021; B. Station classification results 3 in 2022

Hard coral consisted of 9 types: Coral Submassive (CS) 49.38%, Acropora Branching (ACB) 0.72%, Acropora Encrusting (ACE) 1.77%, Acropora Submassive (ACS) 20.6%, Acropora Tabulate (ACT) 1.83%, Coral Branching (CB) 5.04%, Coral Foliose (CF) 0.98%, Coral Massive (CM) 1.11%, and Coral Mushroom (CMR) 0.33%. At Station 3, Hard Coral Life was 45.46%, Soft Coral 0%, Others 4.31%, Mobile Substrate 37.47%, and Available Substrate 12.76% (Table 2). Hard coral included 8 types, dominated by Acropora Submassive (ACS) 17.92%, Acropora Branching (ACB) 1.9%, Acropora Encrusting (ACE) 1.18%, Coral Branching (CB) 0.07%, Coral Foliose (CF) 2.09%, Coral Massive (CM) 8.63%, Coral Mushroom (CMR) 0.52%, and Coral Submassive (CS) 13.15%.

Discussion

In recent years, the use of drone for coastal mapping has experienced substantial progress with diverse applications. The use of drone includes mapping small islands, mapping mangroves (Ruwaimana et al. 2018), mapping coral reefs (Casella et al. 2017), topography mapping (Kullmann 2017), land mapping (Rossi et al. 2018), and marine habitat mapping (Ventura et al. 2016). The advantages of using drone include higher orthophoto-mosaic resolution compared to commercially available satellite images such as WorldView-2, commonly used for coral reefs mapping (Sugara et al. 2020). Therefore, larger coral, genera, or different growth forms can be distinguished more effectively. Furthermore, high-resolution drone surveys can be repeated multiple times, facilitating real-time monitoring of changes in coral cover and events such as coral bleaching. These changes can be detected and correlated with information about coral morphology. This is a valuable method for monitoring disturbances, such as coral bleaching or outbreaks of *Acanthaster planci*, through fixed aerial transects or the presence of grazing halos as indicators of predator loss. This is in line with the results of Kabiri et al. (2020) who conducted coral reefs mapping using drone equipped with multispectral cameras, along with Ground Control Points (GCPs) to improve planimetric accuracy. While this method significantly improves capabilities, it comes with an increased cost.

This research shows that the use of drone for coral reefs mapping in shallow waters can use the supervised maximum likelihood classification method temporarily. The results of drone image mapping using the Maximum Likelihood algorithm can be utilized to observe coral reef growth by analyzing changes in their coverage. At Station 1, there was an increase in live coral coverage by 146.41 m^2 (26.48%). The most significant growth was observed in Porites corals, increasing from 5.38% to 14.55%. The rapid growth of Porites corals is attributed to their ability to survive under various un-favorable environmental conditions, such as high sedimentation and fluctuating salinity levels. Darling et al. (2012) emphasize that life-history traits determine recovery potential, with species exhibiting high stress tolerance (e.g. Porites) showing post-disturbance increases. Porites tend to be more resilient to environmental disturbances, such as fluctuations in salinity and high sedimentation, thus enabling them to recover or even grow better after a disturbance. At Station 2, a decline in live coral coverage was recorded, reaching 277.64 m^2 (27.53%). The most significant reduction was seen in Acropora corals, which decreased by 172.63 m^2 (17.39%). Meanwhile, rubble at Station 2 increased by 289.05 m^2 (30.07%), indicating a substantial loss of live coral. Hughes et al. (2018) noted that species such as Acropora, which are branching corals, are highly susceptible to thermal and physical disturbances, often experiencing dramatic declines. An increase in rubble areas has also been reported in studies observing the impact of physical disturbances and the accumulation of coral fragments due to structural damage. At Station 3, despite having a high percentage of live coral, there was a reduction in live coral coverage of 44.67 m^2 (8.66%).

Table 3. Percentage of coral cover at each measurement station using the Underwater Photo Transect (UPT) method

Description	Percentage cover (%)		
	Station 1	Station 2	Station 3
Hard Coral Life			
Acropora Branching (ACB)	30.61	0.72	1.9
Acropora Digitate (ACD)	0.94	0	0
Acropora Encrusting (ACE)	0	1.77	1.18
Acropora Submassive (ACS)	5.61	20.6	17.92
Acropora Tabulate (ACT)	0	1.83	0
Coral Brancing (CB)	4.88	5.04	0.07
Coral Encrusting (CE)	0.13	0	0
Coral Foliose (CF)	3.14	0.98	2.09
Coral Heliopora (CHL)	0	0	0
Coral Milepora (CME)	0	0	0
Coral Massive (CM)	7.09	1.11	8.63
Coral Mushroom (CMR)	2.01	0.33	0.52
Coral Submassive (CS)	0.53	49.38	13.15
Coral Tubipora (CTU)	0	0	0
Total	54.94	81.76	45.46
Soft Coral Life			
Soft Coral	0.07	2.75	0
Other			
Biota	0.2	0.07	3.79
Sponge	0	0	0
Anemon			
Alga	0.27	1.44	0.52
Total	0.47	1.51	4.31
Mobile Substrate			
Rubble	14.1	4.32	29.95
Sand	2.34	2.81	7.52
Silt	0	0	0
Total	16.44	7.13	37.47
Available Substrate			
Rock	0	0	0.13
Dead Coral	2.34	4.77	9.88
Dead Coral with algae	25.74	2.09	2.75
Total	28.08	6.86	12.76

Figure 6. Coral reef photographs using the Underwater Photo Transect (UPT) method at A. Station 1; B. Station 2; C. Station 3

The largest decrease was observed in Acropora corals, which declined by 93.10 m^2 (20.71%). On the other hand, Goniastrea, Mycedium, and Porites species showed increases, while Stylophora experienced a decline. Rubble at Station 3 also increased by 37.32 m^2 (8.57%), suggesting some degree of coral damage, although not as extensive as at Station 2. Darling et al. (2012) further demonstrated that there are distinct dynamics among species; more sensitive species (e.g. Acropora and Stylophora) tend to decline under disturbance conditions, whereas more tolerant species (such as Porites) can maintain or even enhance their presence. The accuracy test using the confusion matrix resulted in an overall accuracy ranging from approximately 74.20% to 86.47% (2021) and 79.94% to 90.87% (2022) respectively. The kappa coefficient values obtained were 71.80% to 82.72% (2021) and 70.33% to 89.25% (2022). The reported accuracy and kappa values are consistent with studies that utilize remote sensing techniques for coral mapping. For instance, Hedley et al. (2016) explained that the challenge of achieving consistent accuracy is greatly influenced by variability in environmental conditions and differences in image processing methodologies. Research findings indicate varied responses among stations: an increase in live coral at Station 1 (dominated by Porites), a significant decline at Station 2 (with a sharp decrease in Acropora and an increase in rubble), and mixed dynamics at Station 3, which are in line with previous study findings. These differences are primarily attributed to local environmental conditions (sedimentation, salinity, physical/anthropogenic disturbances), species characteristics (stress tolerance), and methodological differences in data observation and analysis.These values are in line with the results of Ventura et al. (2016) which reported Overall Accuracy for Maximum Likelihood ranging from 78.78% to 80.18%. This also explains that drone is easy to use, cost-effective, and timely in capturing aerial photos of marine areas. In addition, various methods were applied in this research including the modern algorithm of semi-automatic image analysis and classification (Maximum Likelihood, ECHO, and Object-based Image Analysis). The results show that these methods have the potential for mapping and monitoring coastal marine habitats, with overall accuracy for maximum likelihood ranging from 78.78% to 80.18%, Extraction and Classification of Homogeneous Objects (ECHO) achieving 80-81.33%, and object-based image analysis reaching 89.01%.

Husson et al. (2016) also conducted research using object-based image analysis with two classification methods namely threshold classification and Random Forest. The results showed that the threshold classification had an overall accuracy ranging from 93% to 99%, while the Random Forest classification ranged from 56% to 94%. Subsequently, this research explains that the automatic classification of aquatic vegetation has great potential for operational mapping of aquatic vegetation. In another result, Collin et al. (2018) integrated the technology of LiDAR bathymetry systems with a passive multispectral camera mounted on drone to map the ecological conditions of coral reefs at a submeter scale. The aerial drone values (pixel size 0.03 m) were used to calibrate the surface data and the airborne LiDAR bathymetry intensity (pixel size 0.5 m). The classification used an Artificial Neural Network (ANN), and the overall accuracy obtained was 75%. Meanwhile, Casella et al. (2017) compared Digital Elevation Model (DEM) data from drone bathymetry with LiDAR data for coral reefs. The results concluded that under calm water conditions, gentle winds, and minimal sunlight, consumer-grade drone could be used for relatively inexpensive and rapid surveys to produce multispectral and bathymetric data for shallow coral reefs. Therefore, these methods are highly useful for monitoring temporal changes in reefs topography complexity and related biological processes.

Zapata-Ramírez et al. (2023) explained that using drone imagery for coral reef management begins with the selection of orthomosaics and the classification of coral reef habitats into four categories: coral, macroalgae, sand, and rubble. These classes can be effectively mapped using various Machine-Learning (ML) algorithms. This method is user-friendly and suitable for monitoring coral reef ecosystems. Differences in accuracy values may arise due to variations in the number of classes used in the classification. On the other hand, that images using true color in vegetation classification may have nearly identical spectral values, leading to lower accuracy. Casella et al. (2017), achieving an Overall Accuracy (OA) value of 75% is considered strong accuracy, given the variability of coral reefs condition. Hossain and Chen (2019) further explain that the image quality of a given imagery can significantly

influence whether accuracy values are high or low. Stone et al. (2024) used drone imagery for coral reef surveys, classified using a segmentation method with an average accuracy of 70-75%. Bennett et al. (2020) achieved a classification accuracy of 86% and mapped live coral cover with an accuracy of 92%. Giles et al. (2023) achieved a precision of 0.96 and a Jaccard index of 0.89 in the classification of non-bleached corals. This method reached a prediction precision of 76% in image areas with more than 2,000 bleached corals.

The percentage of live coral cover is classified as follows: 75-100% is categorized as very good, 50-74.9% as good, 25-49.9% as fair, and 0-24.9% as bad (Pelasula et al. 2021). The percentage of coral cover at Gili Labak Island, based on a survey using the underwater photo transect method, showed an average live coral cover of 61.66%, falling under the good category. At station one, the coral cover was 55.01% (good), station two was 81.79% (very good), and station three was 45.46% (fair). This indicates that coral reef ecosystem conditions vary between stations. Factors contributing to the resilience of coral reef ecosystems include ecosystem condition, biodiversity, regional connectivity, and local environmental conditions. Currents can influence coral growth forms; the higher the hydrodynamic pressure, the more likely corals will adopt a hardened growth form. Submassive Coral (CS) is a type of coral that can adapt to extreme aquatic environments.

In conclusion, the supervised Maximum Likelihood algorithm classification can be utilized to observe coral reef growth by analyzing changes in their coverage. At Station 1, live coral coverage increased by 26.48%; at Station 2, it decreased by 27.53%; and at Station 3, it decreased by 8.66%. The accuracy of the supervised Maximum Likelihood algorithm classification ranged from 74.20% to 90.87%, with an average of 82.87%. The kappa coefficient values ranged from 70.33% to 89.25%, with an average of 78.52%. The percentage of live coral cover, based on the underwater photo transect method, averaged 61.66% (categorized as good), with Station 1 at 55.01% (good), Station 2 at 81.79% (very good), and Station 3 at 45.46% (fair). The utilization of drone imagery with the supervised Maximum Likelihood classification method has proven effective for monitoring coral reef growth periodically. This data can be valuable for coral reef conservation efforts.

ACKNOWLEDGEMENTS

We are grateful the Directorate of Research, Technology and Community Service, The Institute for Research and Community Service, Universitas Trunojoyo, Madura, Indonesia has provided this research.

REFERENCES

Ahmad A, Kalsom U, Hashim M. 2018. Comparative analysis of support vector machine, maximum likelihood and neural network classification on multispectral remote sensing data. Intl J Adv Comput Sci Appl 9 (9): 529-537. DOI: 10.14569/IJACSA.2018.090966.

Barrera-Falcon E, Rioja-Nieto R, Hernández-Landa RC, Torres-Irineo E. 2021. Comparison of standard caribbean coral reef monitoring protocols and underwater digital photogrammetry to characterize hard coral species composition, abundance and cover. Front Mar Sci 8: 1-13. DOI: 10.3389/fmars.2021.722569.

Bennett MK, Younes N, Joyce K. 2020. Automating drone image processing to map coral reef substrates using google earth engine. Drones 4: 1-13. DOI: 10.3390/drones4030050.

Burns JHR, Fukunaga A, Pascoe K, Craig B. 2019. 3D habitat complexity of coral reefs in the Northwestern Hawaiian Islands is driven by coral assemblage structure. Intl Arch Photogramm Remote Sensing Spati Inform Sci 42 (10): 61-67. DOI: 10.5194/isprs-archives-XLII-2-W10-61-2019.

Casella E, Collin A, Harris D, Ferse S, Bejarano S, Parravicini V, Hench JL, Rovere A. 2017. Mapping coral reefs using consumer-grade drones and structure from motion photogrammetry techniques. Coral Reefs 36: 269-275. DOI: 10.1007/s00338-016-1522-0.

Collin A, Ramambason C, Pastol Y, Casella E, Rovere A, Thiault L, Espiau B, Siu G, Lerouvreur F, Nakamura N. 2018. Very high resolution mapping of coral reef state using airborne bathymetric LiDAR surface-intensity and drone imagery. Intl J Remote Sensing 39 (17): 5676-5688. DOI: 10.1080/01431161.2018.1500072.

Darling ES, Alvarez-Filip L, Oliver TA, Mcclanahan TR, Côté IM. 2012. Evaluating life-history strategies of reef corals from species traits. Ecol Lett 15 (12): 1378-1386. DOI: 10.1111/j.1461-0248.2012.01861.x.

de Oliveira LMC, Lim A, Conti LA, Wheeler AJ. 2021. 3D classification of cold-water coral reefs: A comparison of classification techniques for 3D Reconstructions of cold-water coral reefs and seabed. Front Mar Sci 8: 1-19. DOI: 10.3389/fmars.2021.640713.

Fukunaga A, Burns JHR, Craig BK, Kosaki RK. 2019. Integrating three-dimensional benthic habitat characterization techniques into ecological monitoring of coral reefs. J Mar Sci Eng Artic 7 (27): 1-13. DOI: 10.3390/jmse7020027.

Giles AB, Ren K, Davies JE, Abrego D, Kelaher B. 2023. Combining drones and deep learning to automate coral reef assessment with RGB imagery. Remote Sensing 15 (9): 1-16. DOI: 10.3390/rs15092238.

Hedley JD, Roelfsema CM, Chollett I, Harborne AR, Heron SF, Weeks SJ, Skirving WJ, Strong AE, Mark EC, Christensen TRL, Ticzon V, Bejarano S, Mumby PJ. 2016. Remote sensing of coral reefs for monitoring and management: A review. Remote Sensing 8 (2): 1-40. DOI: 10.3390/rs8020118.

Hidayat SA, Ayuningtias A, Cahyaningrum YM, Astrida N, Kusumo S. 2023. Temporal study of coral reef health in Kepulauan Seribu Marine National Park. Proceeding of 2nd International Symposium on Aquatic Sciences and Resources Management. Bogor, 22-24 Agustus 2022. [Indonesian]

Hossain MD, Chen D. 2019. Segmentation for Object-Based Image Analysis (OBIA): A review of algorithms and challenges from remote sensing perspective. J Photogramm Remote Sensing 150: 115-134. DOI: 10.1016/j.isprsjprs.2019.02.009.

Hughes TP, Kerry JT, Baird AH, Connolly SR, Dietzel A, Eakin CM, Heron SF, Hoey AS, Hoogenboom MO, Liu G, McWilliam MJ, Pears RJ, Pratchett MS, Skirving WJ, Stella JS, Torda G. 2018. Global warming transforms coral reef assemblages. Nature 556 (7702): 492-496. DOI: 10.1038/s41586-018-0041-2.

Husson E, Ecke F, Reese H. 2016. Comparison of manual mapping and automated object-based image analysis of non-submerged aquatic vegetation from very-high-resolution UAS images. Remote Sensing 8: 1-18. DOI: 10.3390/rs8090724.

lkhrachy I. 2021. Accuracy assessment of low-cost Unmanned Aerial Vehicle (UAV) photogrammetry. Alex Eng J 60 (6): 5579-5590. DOI: 10.1016/j.aej.2021.04.011.

Insafitri I, Asih ENN, Nugraha WA. 2021. The impact of snorkeling on percentage of coral cover at Gili Labak Island, Sumenep Madura. Buletin Oseanografi Marina 10 (2): 151-161. DOI: 10.14710/buloma.v10i2.30160.

Irawan D, Mukti AT, Andriyono S, Muhsoni FF. 2023. Three-dimensional (3D) modelling to determine the weight of massive corals in Gili Labak Island, Sumenep, Madura, East Java, Indonesia. Biodiversity 24 (1-2): 23-33. DOI: 10.1080/14888386.2023.2184425.

Jericho A, Mendoza, Verzosa ALR, Ayop AN. 2023. Evaluation of coral reef health status in the fish sanctuary of San Esteban, Ilocos Sur. Intl J Emerg Sci Technol Manag 32 (1): 36-50. DOI: 10.69566/ijestm.v32i1.302.

Kabiri K, Rezai H, Moradi M. 2020. A drone-based method for mapping the coral reefs in the shallow coastal waters - case study: Kish Island, Persian Gulf. Earth Sci Inform 13 (4): 1265-1274. DOI: 10.1007/s12145-020-00507-z.

Kullmann K. 2017. The drone's eye: Applications and implications for landscape architecture. Landsc Res 43: 906-921. DOI: 10.1080/01426397.2017.1386777.

Li J, Fabina NS, Knapp DE, Asner GP. 2020. The sensitivity of multi-spectral satellite sensors to benthic habitat change. Remote Sensing 12 (3): 20-22. DOI: 10.3390/rs12030532.

Magel JMT, Burns JHR, Gates RD, Baum JK. 2019. Effects of bleaching-associated mass coral mortality on reef structural complexity across a gradient of local disturbance. Sci Rep 9 (1): 1-12. DOI: 10.1038/s41598-018-37713-1.

Martínez-Carricondo P, Agüera-Vega F, Carvajal-Ramírez F, Mesas-Carrascosa FJ, García-Ferrer A, Pérez-Porras FJ. 2018. Assessment of UAV-photogrammetric mapping accuracy based on variation of ground control points. Intl J Appl Earth Obs Geoinform 72: 1-10. DOI: 10.1016/j.jag.2018.05.015.

Nakajima R, Nakayama A, Yoshida T, Kushairi MRM, Othman BHR, Toda T. 2010. An evaluation of Photo Line-Intercept Transect (PLIT) method for coral reef monitoring. Galaxea 12: 37-44. DOI: 10.3755/galaxea.12.37.

Oberle FKJ, Storlazzi CD, Cheriton OM, Takesue RK, Hoover DJ, Logan JB, Runyon C, Kellogg CA, Johnson CD, Swarzenski PW. 2019. Physicochemical controls on zones of higher coral stress where black band disease occurs at Mākua Reef, Kaua'i, Hawai'i. Front Mar Sci 6: 1-16. DOI: 10.3389/fmars.2019.00552.

Pelasula DD, Alik R, Ruli F, Hukom FD, La Pay, Hehuat J. 2021. A coral reef health study and its problem in Leti, Moa and Wetar Island, Mollucas Province. Proceeding of the Second Maluku International Conference on Marine Science and Technology. Ambon, 14 November 2020. DOI: 10.1088/1755-1315/777/1/012003. [Indonesian]

Peng J, Li L, Tang YY, Fellow L. 2018. Maximum likelihood estimation-based joint sparse representation for the classification of hyperspectral remote sensing images. Trans Neural Netw Learn Syst 30: 1-13. DOI: 10.1109/TNNLS.2018.2874432.

Reverter M, Helber SB, Rohde S, de Goeij JM, Schupp PJ. 2022. Coral reef benthic community changes in the Anthropocene: Biogeographic heterogeneity, overlooked configurations, and methodology. Glob Change Biol 28 (6): 1956-1971. DOI: 10.1111/gcb.16034.

Roelfsema C, Kovacs E, Ortiz JC, Wolff NH, Callaghan D, Wettle M, Ronan M, Hamylton SM, Mumby PJ, Phinn S. 2018. Coral reef habitat mapping: A combination of object-based image analysis and ecological modelling. Remote Sensing Environ 208: 27-41. DOI: 10.1016/j.rse.2018.02.005.

Rossi G, Tanteri L, Tofani V, Vannocci P, Moretti S, Casagli N. 2018. Multitemporal UAV surveys for landslide mapping and characterization. Landslides 15: 1045-1052. DOI: 10.1007/s10346-018-0978-0.

Ruwaimana M, Satyanarayana B, Otero V, Muslim AM, Muhammad Syafiq A, Ibrahim S, Raymaekers D, Koedam N, Dahdouh-Guebas F. 2018. The advantages of using drones over space-borne imagery in the mapping of mangrove forests. Plos One 13: 1-22. DOI: 10.1371/journal.pone.0200288.

Sanfourche M, Le Saux B, Plyer A, Le Besnerais G. 2015. Environment mapping and interpretation by drone. Proceeding of Joint Urban Remote Sensing Event JURSE 2015. Universite de Lausanne. Lausanna, 30 March - 1 April 2015. DOI: 10.1109/JURSE.2015.7120454. [Switzerland]

Sativa DY, Septian IGN, Atmanegara FK. 2021. Benthic habitat mapping using Sentinel-2A satellite imagery in Serewe Bay. Jurnal Biologi Tropis 22: 55-61. DOI: 10.29303/jbt.v22i1.3157.

Schaduw JNW, Kondoy KIF, Manoppo VEN, Luasunaung A, Mudeng J, Pelle WE, Ngangi ELA, Manembu IS, Wantasen AS, Sumilat DA, Rumampuk NDC, Tilaar SO, Manengkey HWA, Lintang R, Walalangi JY, Tampanguma B, Pungus F, Lahabu Y, Sagai B, Mamangkey NNT. 2020. Data on percentage coral reef cover in small islands Bunaken National Park. Data Brief 31: 105713. DOI: 10.1016/j.dib.2020.105713.

Stone A, Hickey S, Radford B, Wakeford M. 2024. Mapping emergent coral reefs: a comparison of pixel- and object-based methods. Remote Sensing Ecol Conserv 10 (2): 1-20. DOI: 10.1002/rse2.401.

Storlazzi CD, van Ormondt M, Chen YL, Elias EPL. 2017. Modeling fine-scale coral larval dispersal and interisland connectivity to help designate mutually-supporting coral reef marine protected areas: Insights from Maui Nui, Hawaii. Front Mar Sci 4: 1-14. DOI: 10.3389/fmars.2017.00381.

Sugara A, Siregar VP, Agus SB. 2020. Benthic habitat classification of shallow water using worldview-2 imagery with in-situ and drone data. Jurnal Ilmu Teknologi Kelautan Tropis 12 (1): 135-150. DOI: 10.29244/jitkt.v12i1.26448.

Takesue RK, Storlazzi CD. 2019. Geochemical sourcing of runoff from a young volcanic watershed to an impacted coral reef in Pelekane Bay, Hawaii. Sci Total Environ 649: 353-363. DOI: 10.1016/j.scitotenv.2018.08.282.

Urbina-Barreto I, Chiroleu F, Pinel R, Fréchon L, Mahamadaly V, Elise S, Kulbicki M, Quod JP, Dutrieux E, Garnier R, Bruggemann JH, Penin L, Adjeroud M. 2021. Quantifying the shelter capacity of coral reefs using photogrammetric 3D modeling: From colonies to reefscapes. Ecol Indic121: 107151. DOI: 10.1016/j.ecolind.2020.107151.

Ventura D, Bruno M, Jona LG, Belluscio A, Ardizzone G. 2016. A low-cost drone based application for identifying and mapping of coastal fish nursery grounds. Estuar Coast Shelf Sci 171: 85-98. DOI: 10.1016/j.ecss.2016.01.030.

Vitousek S, Buscombe D, Vos K, Barnard PL, Ritchie AC, Warrick JA. 2023. The future of coastal monitoring through satellite remote sensing. Camb Prism Coast Futures 1 (10): 1-18. DOI: 10.1017/cft.2022.4.

Wedding LM, Jorgensen S, Lepczyk CA, Friedlander AM. 2019. Remote sensing of three-dimensional coral reef structure enhances predictive modeling of fish assemblages. Remote Sensing Ecol Conserv 5 (2): 150-159. DOI: 10.1002/rse2.115.

Wei J, Wang M, Lee Z, Briceño HO, Yu X, Jiang L, Garcia R, Wang J, Luis K. 2020. Shallow water bathymetry with multi-spectral satellite ocean color sensors: Leveraging temporal variation in image data. Remote Sensing Environ 250: 112035. DOI: 10.1016/j.rse.2020.112035.

Yu F, He B, Li K, Yan T, Shen Y, Wang Q, Wu M. 2021. Side-scan sonar images segmentation for AUV with recurrent residual convolutional neural network module and self-guidance module. Appl Ocean Res 113: 102608. DOI: 10.1016/j.apor.2021.102608.

Žabota B, Kobal M. 2021. Accuracy assessment of uav-photogrammetric-derived products using ppk and gcps in challenging terrains: In search of optimized rockfall mapping. Remote Sensing 13 (19): 1-31. DOI: 10.3390/rs13193812.

Zapata-Ramírez PA, Hernández-Hamón H, Fitzsimmons C, Cano M, García J, Zuluaga CA, Vásquez RE. 2023. Development of a google earth engine-based application for the management of shallow coral reefs using drone imagery. Remote Sensing 15 (14): 3504. DOI: 10.3390/rs15143504.

Zhong H, Duan Y, Tao P, Zhang Z. 2025. Influence of ground control point reliability and distribution on UAV photogrammetric 3D mapping accuracy. Geo-Spat Inform Sci 121: 107151. DOI: 10.1080/10095020.2025.2451204.